Evidence Supporting an Association Between Expression of Major Histocompatibility Complex II by Microglia and Optic Nerve Degeneration During Experimental Glaucoma

Glyn Chidlow, DPhil,† Andreas Ebneter, MD, PhD,‡*
John P.M. Wood, DPhil,† and Robert J. Casson, DPhil, FRANZCO*†*

Aim: We acquired age-matched and sex-matched Sprague-Dawley rats from 2 independent breeding establishments. Serendipitously, we observed that constitutive, and bacterial toxin–induced, expression of major histocompatibility complex (MHC) class II RT1B chain in the uveal tract was much lower in one of the cohorts. Activated microglia are known to upregulate MHC II RT1B expression during optic nerve (ON) degeneration induced by raised intraocular pressure (IOP). We investigated whether, in a model of experimental glaucoma, microglial upregulation of MHC II RT1B was less efficacious and ON degeneration correspondingly less severe in the cohort of rats with low MHC II RT1B expression.

Methods: Experimental glaucoma was induced by lasering the trabecular meshwork using a standard protocol. After 2 weeks of elevated IOP, retinal ganglion cells (RGC) survival, ON degeneration, and microglial responses were determined in both cohorts of rats.

Results: Raised IOP-induced expression of MHC II RT1B by microglia was muted in the "Low" cohort compared with the "High" cohort. Axonal degeneration, RGC loss, and microgliosis were all significantly lower in the cohort of rats with low basal and induced expression of MHC II RT1B, despite both cohorts displaying IOP responses that were indistinguishable in terms of peak IOP and IOP exposure.

Conclusions: Expression of MHC II RT1B by activated microglia in the ON during experimental glaucoma was associated with more severe RGC degeneration. Further studies are needed to elucidate the role of MHC II during experimental glaucoma.

Key Words: microglia, major histocompatibility complex, optic nerve, neurodegeneration

(*J Glaucoma* 2016;25:681–691)

There is increasing recognition that glial cells in general, and microglia in particular, play important roles in the survival or death of retinal ganglion cells (RGCs) during glaucoma.[1–4] Microglia serve as the resident immune cells of the CNS, constantly surveying the environment and responding rapidly to disruption of local tissue homeostasis. Neuronal damage triggers microglia to adopt a reactive phenotype that encompasses multiple changes including proliferation, migration, phagocytosis of dying neurons, stimulation of neuroinflammatory pathways, and antigen presentation.[3,5] It has indisputably been proven that microglia within the retina and optic nerve (ON) become reactive in response to RGC degeneration in animal models of glaucoma.[3,6,7] Of arguably greater interest, however, is the recent finding that alterations in microglial function may, in fact, precede RGC injury in glaucoma.[8,9] This result further focuses debate on whether microglial activation is detrimental or beneficial to RGC survival. In support of the hypothesis that reactive microglia are harmful to vulnerable RGCs is the body of evidence demonstrating that suppression of microglial activity is neuroprotective to RGCs in models of experimental glaucoma.[10–14]

The principal route by which microglia induce an immune response is through expression of major histocompatibility complex (MHC) class II.[15] Microglial MHC II is immunohistochemically undetectable in healthy neuronal tissue, but expression is upregulated in response to neurodegenerative signals. Interestingly, an association has been uncovered between MHC II genes and CNS neurodegeneration. Strain-dependent differences in susceptibility to experimental allergic encephalomyelitis (EAE),[16] ventral root avulsion,[17] and axonal injury–induced neuropathic pain[18] have all been linked to differential expression of the RT1B chain of MHC II. Furthermore, mouse MHC II knockout models demonstrate reduced axonal injury in EAE[19] and globoid cell leukodystrophy,[20] and minimal dopaminergic neuron loss in a model of Parkinson disease.[21] The combined data suggest that MHC II expression triggers a greater vulnerability to CNS injury.

While conducting a study investigating proinflammatory events in the eye, we acquired age-matched and sex-matched Sprague-Dawley rats from 2 independent breeding establishments. In a serendipitous finding, we observed that constitutive, and bacterial toxin–induced, expression of MHC II RT1B in the uveal tract was much lower in one of the cohorts. We have previously shown that activated microglia upregulate expression of MHC II RT1B during axonal degeneration induced by ocular hypertension.[22] As an increasing body of evidence supports the theory that activated microglia contribute to disease progression during glaucoma, and as MHC II RT1B expression is both a signature event in reactive microgliosis and is associated with neuronal injury elsewhere within the nervous system, we hypothesized that microglial upregulation of MHC II RT1B would be less efficacious and ON

Received for publication March 30, 2015; accepted April 28, 2016.
From the *Ophthalmic Research Laboratories, South Australian Institute of Ophthalmology, Hanson Institute Centre for Neurological Diseases; †Department of Ophthalmology and Visual Sciences, University of Adelaide, Adelaide, SA, Australia; and ‡Department of Ophthalmology, Bern University Hospital and University of Bern, Inselspital, Bern, Switzerland.
Supported by the NHMRC (project grant: APP1050982) and the Ophthalmic Research Institute of Ophthalmology.
Disclosure: The authors declare no conflict of interest.
Reprints: Glyn Chidlow, DPhil, Ophthalmic Research Laboratories, South Australian Institute of Ophthalmology, Hanson Institute Centre for Neurological Diseases, Frome Rd, Adelaide, SA 5000, Australia (e-mail: glyn.chidlow@health.sa.gov.au).

DOI: 10.1097/IJG.0000000000000447

degeneration during experimental glaucoma would be correspondingly less severe in the colony of rats with low MHC II RT1B expression. The present study tested this hypothesis.

METHODS

Experimental Plan

There were 3 phases to the overall study:

(1) Basal expression of MHC II RT1B: We obtained 2 cohorts of age-matched, female rats. These were as follows: Sprague-Dawley rats (Animal Resources Centre, Perth; n = 7) and Sprague-Dawley rats (Adelaide University, Adelaide; n = 7). Basal expression of MHC class II invariant chain (CD74) and MHC II RT1B chain (Ia antigen; OX-6) within the uveal tract was assessed in each cohort of rats.

(2) Induced expression of MHC II RT1B: In phase 2, expression of MHC class II invariant chain and MHC II RT1B chain within the uveal tract was assessed in both cohorts of rats at 24 hours following intravitreal injection of the proinflammatory endotoxin lipopolysaccharide (LPS) (n = 5).
Results of phases 1 and 2 demonstrated that expression of MHC II RT1B was substantially lower in Sprague-Dawley rats from Animal Resources Centre, Perth as compared with Sprague-Dawley rats from Adelaide University, Adelaide. As a consequence, we proceeded to phase 3 in which we tested the hypothesis that ON degeneration during experimental glaucoma would be less severe in the colony of Sprague-Dawley rats with low MHC II RT1B expression than in the colony of Sprague-Dawley rats with phenotypically higher expression.

(3) Experimental glaucoma: Adult, female Sprague-Dawley rats (n = 28) from the colony with higher MHC II RT1B (Adelaide University, Adelaide) were designated cohort "High." Age-matched and sex-matched rats (n = 28) from the colony with lower expression of MHC II RT1B (Animal Resources Centre, Perth) were designated cohort "Low." Ocular hypertension was then induced in the right eye of all animals. To characterize intraocular pressure (IOP) profiles for each rat, peak IOP, IOP integral (area under the curve of the lasered eye), and the IOP exposure (area under the curve of the lasered eye minus area under the curve of control eye) were calculated. After 14 days, ONs and retinas were analyzed for severity of RGC injury and for expression of microglial markers.

Animals and Procedures

This study was approved by the SA Pathology/CHN Animal Ethics committee and conforms with the Australian Code of Practice for the Care and Use of Animals for Scientific Purposes, 2004. All procedures were performed under appropriate anesthesia and care was taken to minimize suffering. All experiments also conformed to the ARVO Statement for the Use of Animals in Ophthalmic and Vision Research. Adult Sprague-Dawley rats (220 to 300 g) were housed in a temperature-controlled and humidity-controlled environment with a 12-hour light, 12-hour dark cycle, and were provided with food and water ad libitum.

Endotoxin-induced Uveitis

Rats were anesthetized with isoflurane during which time an intravitreal injection of 0.2% LPS (5 μL in sterile saline) was performed in 1 eye. The contralateral eye was untreated. All rats were killed after 24 hours.

Experimental Glaucoma

Rats were anesthetized with 100 mg/kg ketamine and 10 mg/kg xylazine and local anesthetic drops were applied to the eye. Ocular hypertension was then induced in the right eye of each animal by laser photocoagulation of the trabecular meshwork using a slightly modified protocol[22] of the method described by Levkovitch-Verbin et al.[23] A second laser treatment was given on day 7 if the difference in IOP between the 2 eyes was < 8 mm Hg. After brief anesthesia with isoflurane, IOPs were measured in both eyes at baseline, day 1, 3, 7, 10, and 14 using a rebound tonometer, factory calibrated for use in rats. One rat from each cohort failed to demonstrate an adequate IOP elevation (minimum increase in IOP of 10 mm Hg) and these rats were excluded from the study. In addition, 2 rats from the High cohort and 1 rat from the Low cohort were excluded due to hyphema, whereas 1 rat each from the High and Low cohorts died under anesthesia. As a result, the High and Low cohorts comprised n = 24 and n = 25 rats that contributed to the final analysis.

Tissue Processing and Immunohistochemistry

All rats were killed by transcardial perfusion with physiological saline under deep anesthesia. Both eyes, both ONs and the optic chiasm were carefully dissected. From the dissected tissue, a short piece of ON, 1.5 mm behind the globe, was removed for resin processing and subsequently toluidine blue staining as previously reported.[22] Tissues taken for immunohistochemistry were fixed in 10% buffered formalin for at least 24 hours and then processed for routine paraffin-embedded sections. Globes were embedded sagitally and chiasmata longitudinally. In all cases, 4-μm serial sections were cut using a rotary microtome.

Colorimetric immunohistochemistry was performed as previously described.[24,25] Briefly, tissue sections were deparaffinized and endogenous peroxidase activity was blocked with H_2O_2. Antigen retrieval was performed by microwaving sections in 10 mM citrate (pH 6.0) and nonspecific labeling blocked with PBS containing 3% normal horse serum (PBS-NHS). Sections were incubated overnight at room temperature in primary antibody (in PBS-NHS), followed by consecutive incubations with biotinylated secondary antibody (Vector, Burlingame, CA) and streptavidin-peroxidase conjugate (Pierce, Rockford, IL). Color development was achieved using 3′-,3′-diaminobenzidine for 5 minutes. Sections were counterstained with hematoxylin, dehydrated, cleared in histolene, and mounted. Confirmation of the specificity of antibody labeling was judged by the morphology and distribution of the labeled cells, by the absence of signal when the primary antibody was replaced by isotype/serum controls, and by comparison with the expected staining pattern based on our own, and other, previously published results. All of the antibodies used in the current study have previously been validated for use in the retina.

The following primary antibodies were used in the study: mouse anti-NeuN (1:1500, clone A60; Merck Millipore), rabbit anti-ionized calcium-binding adapter molecule-1 (iba1, 1:20,000, Cat# 019-19741; Wako), mouse anti-CD68

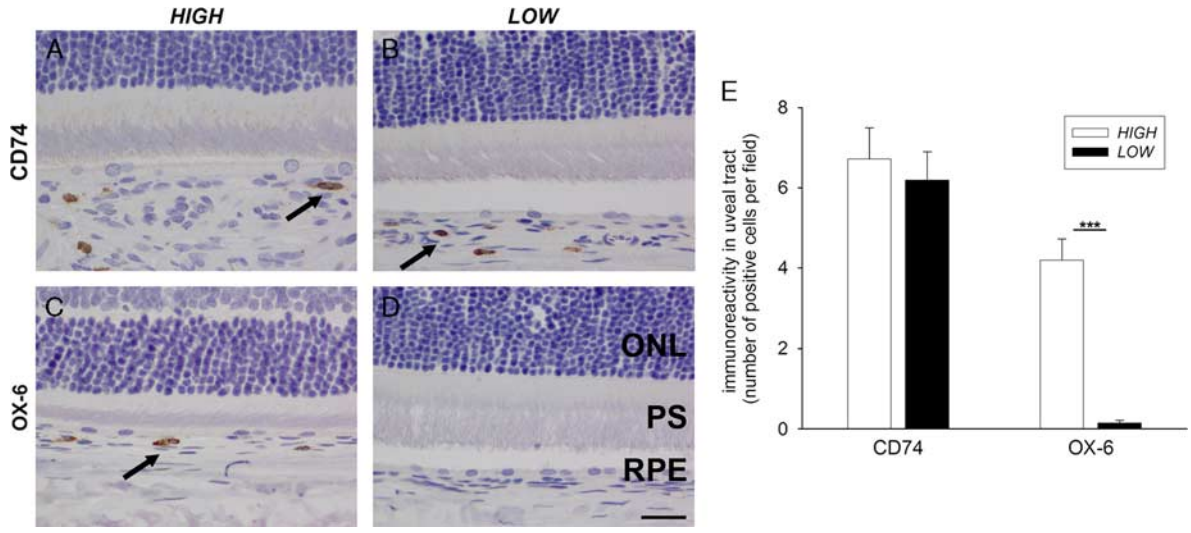

FIGURE 1. Expression of MHC class II invariant chain (CD74) and MHC II RT1B chain (Ia antigen; OX-6) within the uveal tract of 2 discrete cohorts of age-matched, female rats. A–D, Example photomicrographs of CD74-positive (A, B) and OX-6-positive (C, D) cells in the choroid of both cohorts. The cohorts were designated High and Low with regard to their basal expression of OX-6. Scale bar: 25 μm. E, Quantification of CD74 and OX-6 expression within the uveal tract in the High and Low cohorts. Values are expressed as mean ± SEM, where n = 7. ***$P < 0.001$ by Mann-Whitney test (OX-6 data are not normally distributed). Example photomicrographs of CD74-positive (A, arrow; B, arrow) and OX-6-positive (C, arrow; D) cells in the choroid of both cohorts. MHC indicates major histocompatibility complex; ONL, outer nuclear layer; PS, photoreceptor segments; RPE, retinal pigment epithelium.

(1:500, clone ED1; AbDSerotec), mouse anti-MHC II RT1B chain (1:400, OX-6; AbDSerotec), and goat anti-CD74 (1:1000, Cat# sc-5438; Santa-Cruz).

Evaluation of Immunohistochemistry

Immunolabeling for each antigen was performed in a single batch and all analyses were conducted in a blinded manner. Evaluations were by 2 independent observers.

Uveal Tract (Phases 1 and 2 of the Study)

Immunohistochemistry for CD74 and OX-6 was performed using sections of the whole globe. For each animal, 1 photomicrograph was taken from the iris, the ciliary body, and the choroid using the ×20 microscope objective. The number of positively labeled cells in each photomicrograph was determined. Measurements from the 3 uveal areas of each animal were averaged and treated as an independent data point.

RGC Survival (Phase 3 of the Study)

Two sections from each animal were stained and quantified for NeuN. To minimize sampling errors, all analyses were performed on sections taken at the level of the ONH. RGCs, immunostained for NeuN, were counted across the entire retina from ciliary body to ciliary body. RGC loss was calculated by comparing the glaucomatous right eye of each animal to the normotensive left eye. NeuN has been shown to be a robust marker of RGCs and has been used in numerous studies evaluating RGC survival. The potential drawback with NeuN is that it also labels displaced amacrine cells; however, amacrine cells have been shown not to die in rodent models of glaucoma, thus, any decrease in NeuN number represents RGC loss.

ON (Phase 3 of the Study)

For each antigen, immunohistochemistry was performed using 1 section of mid ON and 1 section of distal ON adjacent to the optic decussation as previously described.[26] One photomicrograph from each location covering the entire width of the nerve was taken using the ×20 microscope objective. Measurements from 1 animal were averaged and treated as an independent data point. In total, approximately 6% of the ON was sampled for quantification. For iba1, ED1, and CD74, evaluations were performed using the ImageJ 1.42q software package platform (http://rsb.info.nih.gov/ij/). For counterstained sections, color deconvolution was applied to extract the DAB staining. After thresholding, the area of staining was measured. Left ONs served as controls. For OX-6, the number of positive cells per micrographic field was counted manually by a single observer.

Evaluation of Semithin Toluidine Blue–stained ON Cross-Sections

Axon counting was determined using a semi-quantitative, automated, fixed pattern sampling approach as previously described.[27] All evaluations were performed in a blinded manner. Five photomicrographs were taken from each ON cross-section, representing a total sampling area of approximately 6%. Images were contrast enhanced, and each axon with a single, intact myelin sheath was counted using a macroroutine written for ImageJ. The mean count from the 5 photomicrographs was used to extrapolate the number of axons in the cross-section. Axonal loss was calculated by comparing the glaucomatous right ON of each animal to the normotensive left ON.

Statistical Analysis

IOP data are expressed as mean ± SD to reveal the variability or scatter within the dataset. This allows

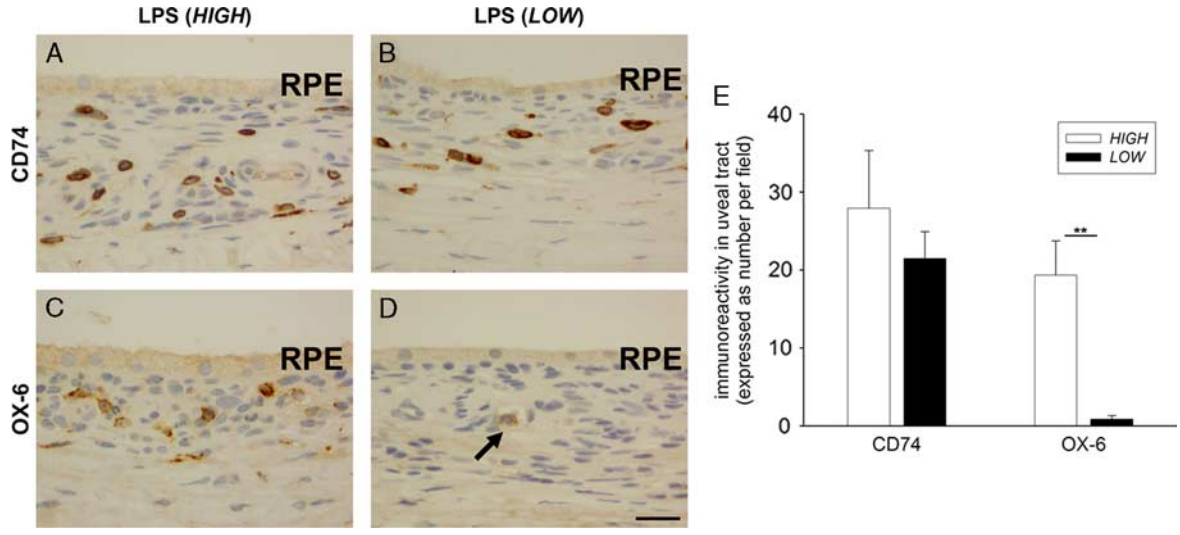

FIGURE 2. Expression of iba1, MHC class II invariant chain (CD74), and MHC II RT1B chain (OX-6) within the High and Low cohorts at 1 day after intravitreal injection of the proinflammatory endotoxin lipopolysaccharide. A, Example photomicrographs of CD74-positive (A, B) and OX-6-positive (C, D) cells in the choroid of both cohorts. Lipopolysaccharide-treated rats from both cohorts showed increased numbers of CD74 cells within the choroid. In the High cohort, numerous OX-6-positive cells are visible within the choroid after lipopolysaccharide treatment. In contrast, OX-6-positive cells are scarce in the Low cohort (arrow). Scale bar: 25 μm. E, Quantification of CD74 and OX-6 expression within the uveal tract in the High and Low cohorts. Values are expressed as mean ± SEM, where n = 5. $^{**}P < 0.01$ by Mann-Whitney test (OX-6 data are not normally distributed). LPS indicates lipopolysaccharide; RPE, retinal pigment epithelium.

inferences to be drawn about the reproducibility of the laser photocoagulation procedure to elevate IOP. All other data are expressed as mean ± SEM, as SEM quantifies the precision of the mean. For statistical testing, an unpaired *t* test was used if parametric assumptions were met (axon loss, NeuN, iba1); a Mann-Whitney test was used otherwise (ED1, CD74, OX-6). Statistical analyses, including correlations, were performed by GraphPad Prism 5.0b (GraphPad Software Inc., La Jolla, CA).

RESULTS

Differential Expression of MHC II RT1B Chain in 2 Cohorts of Sprague-Dawley Rats

We acquired age-matched, female Sprague-Dawley rats from 2 independent breeding establishments. In a serendipitous finding, we anecdotally observed that expression of MHC II RT1B (Ia antigen; OX-6) was much lower in the uveal tract in rats from one of the establishments than in the other. To verify this observation, and further to ascertain whether the lower expression of OX-6 was simply reflective of reduced MHC II expression per se rather than specifically of the RT1B chain, we quantified OX-6 and CD74 immunoreactivities in the uveal tract (iris, ciliary body, and choroid) of rats from both cohorts (Figs. 1A–E). Note that CD74 recognizes the invariant chain of MHC class II. The data showed that both cohorts of rats featured a similar number of CD74-positive cells within the uveal tract ($P = 0.62$), but that the number of OX-6-positive cells was markedly higher in one of the cohorts ($P < 0.001$; Fig. 1E). The cohorts were thus designated High and Low with regard to their basal expression of OX-6.

TABLE 1. IOP Responses in the High and Low Cohorts During Experimental Glaucoma

Cohort	Peak IOP	IOP Exposure	IOP Integral
High (n = 24)	39.1 ± 5.8	167.2 ± 74.5	349.7 ± 76.1
Low (n = 25)	40.6 ± 7.3	191.8 ± 107.9	351.7 ± 108.3
P	0.41	0.36	0.94

Peak IOP is mm Hg ± SD. IOP exposure is total positive integral data in units of mm Hg (mean ± SD). IOP integrals are also in units of mm Hg (mean ± SD).

P-values are given for the comparison between the High and the Low experimental cohorts (Student unpaired *t* test, 2-tailed).

IOP indicates intraocular pressure.

Next, we investigated expression of MHC II within the context of a local inflammatory environment. Intraocular administration of the endotoxin LPS induces a nonspecific ocular inflammation (uveitis) of short duration, which is characterized by an acute infiltration of leukocytes, protein accumulation in the anterior chamber, anterior and posterior segment inflammatory changes, and increased expression of MHC II.[28] In both cohorts of rats, LPS caused ostensibly similar responses typified by anterior and posterior inflammatory changes and increased expression of iba1 (data not shown) and CD74 (Fig. 2A, B) throughout the uveal tract. However, expression of OX-6 was markedly lower in the Low cohort as compared with the High cohort ($P < 0.01$; Figs. 2C–E).

IOP Characteristics in the High and Low Cohorts During Experimental Glaucoma

There was no difference in peak IOP ($P = 0.41$), IOP integral ($P = 0.94$), or IOP exposure ($P = 0.36$) between the Low and High cohorts over the 2-week period of experimental glaucoma (Table 1). IOP values reported are similar to those previously documented by other groups using the same model.[29,30]

Copyright © 2016 Wolters Kluwer Health, Inc. All rights reserved.

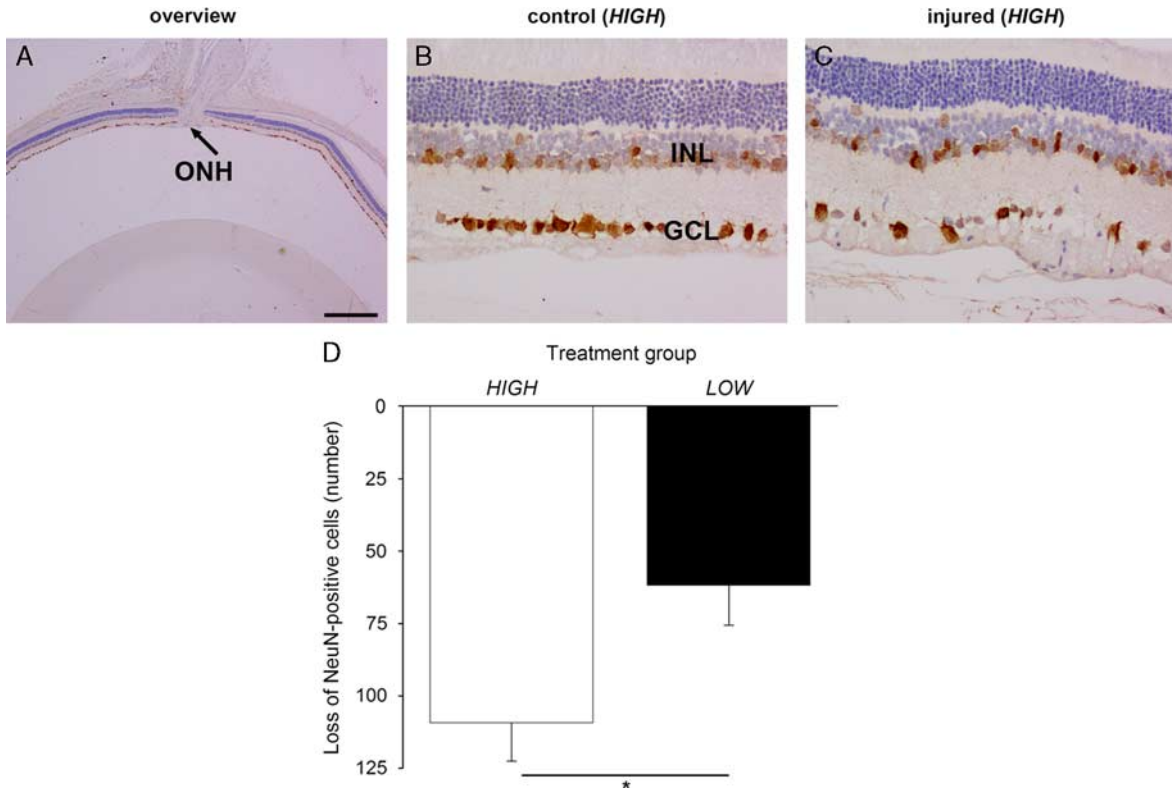

FIGURE 3. Retinal ganglion cell (RGC) survival at 2 weeks after induction of experimental glaucoma in the High and Low cohorts. A–C, Example photomicrographs of transverse sections of retinas immunolabeled for NeuN, featuring overview of posterior eyecup (control eye from High cohort) with position of optic nerve head indicated (A, arrow), control retina from High cohort (B), and injured retina from High cohort (C). Scale bar: A = 500 μm; B, C = 50 μm. D, Estimated loss of NeuN-positive RGCs (untreated left eye minus glaucomatous right eye) in transverse section of retina taken through the optic nerve head. Values are expressed as mean ± SEM, where n = 24-25. $^{*}P < 0.05$ by Student unpaired *t* test. GCL indicates ganglion cell layer; INL, inner nuclear layer; ONH, optic nerve head.

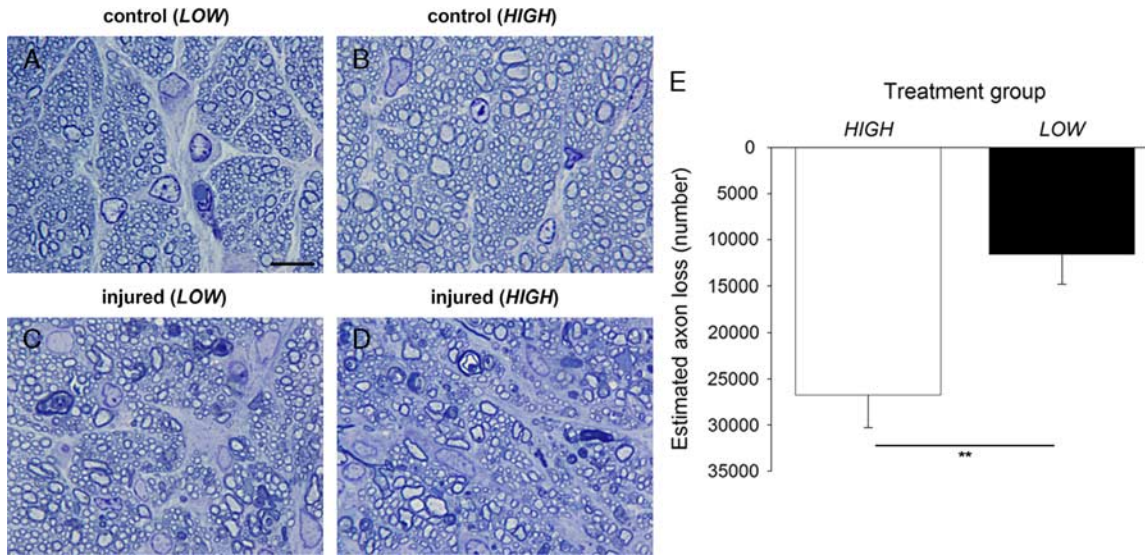

FIGURE 4. Axonal integrity at 2 weeks after induction of experimental glaucoma in the High and Low cohorts. A–D, Example photomicrographs of toluidine blue–stained cross-sections of control optic nerves from the Low (A) and High (B) cohorts, injured optic nerve from the Low cohort (C), and injured optic nerve from the High cohort (D). Scale bar: 10 μm. E, Estimated axon loss (untreated left optic nerve minus glaucomatous right optic nerve) in the Low and High cohorts. Values are expressed as mean ± SEM, where n = 24-25. $^{**}P < 0.01$ by Student unpaired *t* test.

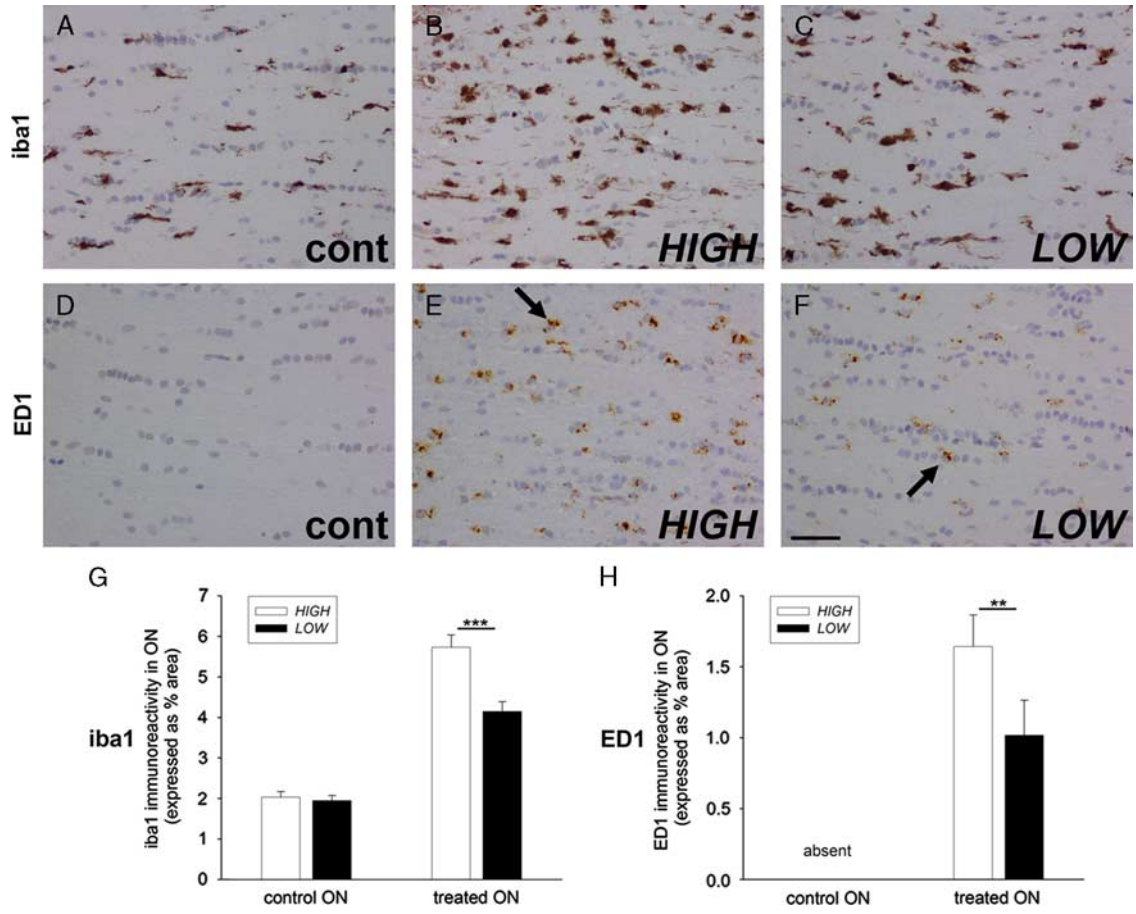

FIGURE 5. Analysis of microglial activation at 2 weeks after induction of experimental glaucoma in the High and Low cohorts. A–F, Representative images of Iba1 and ED1 (arrows) expression in control (cont) optic nerves, and injured optic nerves of the High and Low cohorts. Scale bar: 50 μm. G and H, Quantification of iba1 and ED1 expression in longitudinal segments of the intracranial optic nerve. Values are expressed as mean ± SEM. ***$P < 0.001$ by Student unpaired *t* test (iba1 data are normally distributed); **$P < 0.01$ by Mann-Whitney test (ED1 data are not normally distributed). ON indicates optic nerve.

RGC Loss in the High and Low Cohorts During Experimental Glaucoma

Loss of RGCs was assessed by quantification of NeuN-positive cells in the ganglion cell layer across the entire retina (Figs. 3A–C). NeuN has repeatedly been demonstrated to represent a reliable marker for determining RGC survival in models of RGC degeneration. The mean loss of NeuN-positive cells (glaucomatous eye minus control eye) was 109.4 ± 13.2 in the High cohort versus 61.8 ± 13.7 in the Low cohort (Fig. 3D). This difference was statistically significant ($P = 0.02$).

Axon Loss in the High and Low Cohorts During Experimental Glaucoma

Estimated axon loss was assessed in semithin, toluidine blue–stained transverse sections of the proximal (intraorbital) ON (Figs. 4A–D) using a fixed pattern sampling approach. The mean loss of axons (glaucomatous ON minus control ON) was 26,413 ± 3534 in the High cohort versus 11,596 ± 3229 in the Low cohort (Fig. 4E). This difference was statistically significant ($P < 0.01$).

Microglial Responses in the High and Low Cohorts During Experimental Glaucoma

Microglial number and phagocytic activity in the ON, as detected by labeling for iba1 and ED1, respectively, have been shown to correlate positively with the extent of axonal injury during experimental glaucoma.[22] To verify that ON damage in the High cohort was, on average, greater than that in the Low cohort, we immunolabeled longitudinal segments of the intracranial ON with iba1 and ED1 (Figs. 5A–F). Both markers were significantly ($P < 0.001$ for iba1; $P < 0.01$ for ED1) more abundant in the High cohort compared with the Low cohort (Figs. 5G, H), the extent to which reflected the amount of axonal damage in each cohort.

MHC II Responses in the High and Low Cohorts During Experimental Glaucoma

Minimal expression of CD74 (MHC II invariant chain) was detectable in uninjured ONs of both the High and Low cohorts (Figs. 6A, B). At 2 weeks after induction of experimental glaucoma, however, there was a marked increase in the number of CD74-positive cells in the ONs of both cohorts (Figs. 6C, D). Double labeling showed that

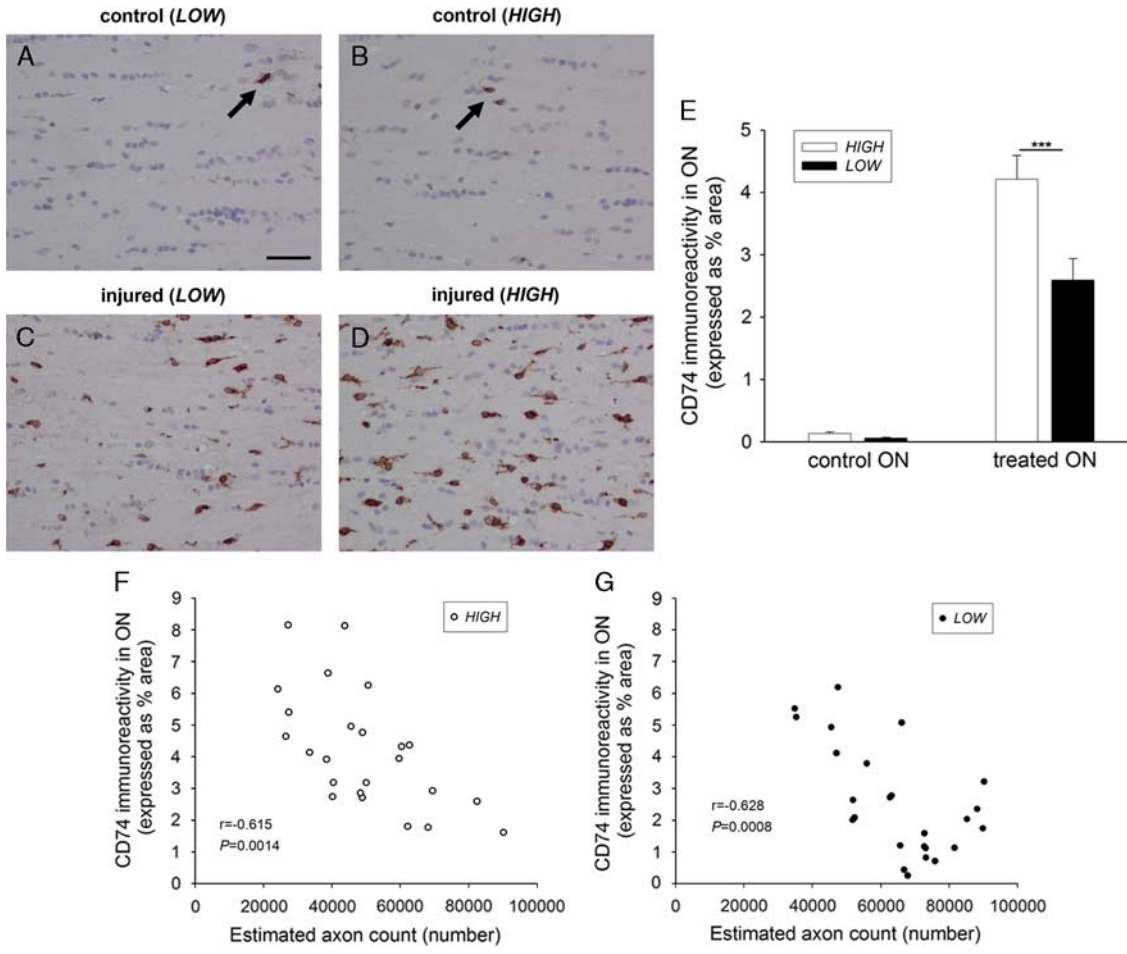

FIGURE 6. Analysis of expression of MHC II invariant chain (CD74) by microglia at 2 weeks after induction of experimental glaucoma in the High and Low cohorts. A–D, Representative images of CD74-positive microglia in control (A, B) and injured (C, D) ONs of the High and Low cohorts. Scale bar: 50 μm. E, Quantification of CD74 expression in longitudinal segments of the intracranial ON. Values are expressed as mean ± SEM. ***$P < 0.001$ by Mann-Whitney test (CD74 data are not normally distributed). F and G, Correlation between estimated axon counts (in transverse sections of the proximal ON) and abundance of CD74 immunoreactivity (in longitudinal sections of the intracranial ON) at 2 weeks after induction of experimental glaucoma in the High (E) and Low (F) cohorts. Each data point represents 1 animal. MHC indicates major histocompatibility complex; ON, optic nerve.

CD74 expression occurred exclusively in iba1-positive microglia (data not shown). Quantification of the relative responses showed that CD74 was significantly ($P < 0.001$) more abundant in the High cohort compared with the Low cohort (Fig. 6E). We were interested in delineating the extent to which the CD74 response reflected the severity of axonal injury; thus, we performed correlations of the estimated axon count with the abundance of CD74 immunoreactivity for each animal (Figs. 6F, G). Analysis of the data revealed a highly significant correlation between the 2 parameters in both cohorts ($P = 0.001$ for the High and Low cohorts). As for iba1 and ED1, expression of CD74 by microglia was proportional to the severity of axonal damage.

Analogous to CD74, there was negligible expression of OX-6 (MHC class II RT1B) in control ON tissue (Figs. 7A, D). At 2 weeks after induction of experimental glaucoma, there was an increase in the number of OX-6-positive cells in the ONs of the High cohort (Figs. 7B, C, G). As for iba1, ED1, and CD74, the extent of OX-6 expression in the High cohort was typically related to the severity of injury (Figs. 7B, C). Indeed, there was an excellent correlation between the CD74 and OX-6 immunoreactivities ($r = 0.75$; $P < 0.001$) in this cohort (Fig. 8A). In contrast, the majority of animals in the Low cohort failed to display a commensurate induction of OX-6 immunoreactivity at 2 weeks after induction of experimental glaucoma with staining absent or weak in virtually all animals (Figs. 7E, F). Quantification of the relative responses showed that OX-6 was dramatically more abundant in the High cohort compared with the Low cohort (Fig. 7G). Scrutiny of the relative abundances of CD74 and OX-6 in the Low cohort revealed minimal expression of OX-6 in animals with mild or moderate damage with somewhat greater expression in the more severely injured ONs (Fig. 8B).

DISCUSSION

In the current study, we compared RGC survival, ON degeneration, and microglial responses following chronic

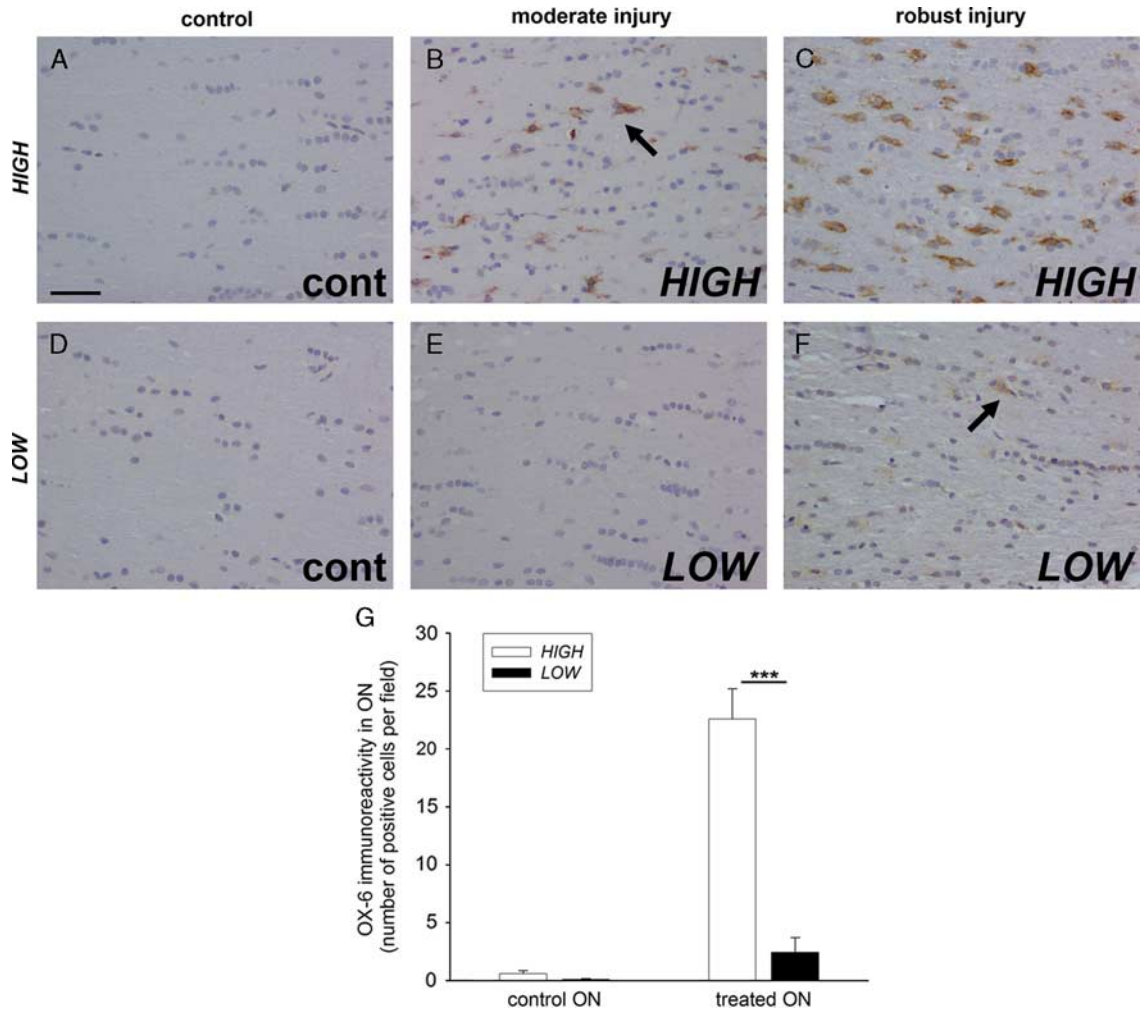

FIGURE 7. Analysis of expression of MHC II RT1B chain (OX-6) by microglia at 2 weeks after induction of experimental glaucoma in the High and Low cohorts. A–F, Representative images of OX-6-positive microglia (arrows) in control (cont) ONs (A, D), moderately injured (B, E), and robustly injured (C, F) ONs of the High and Low cohorts. Scale bar: 50 μm. G, Quantification of OX-6 expression in longitudinal segments of the intracranial ON. Values are expressed as mean ± SEM. ***$P < 0.001$ by Mann-Whitney test (OX-6 data are not normally distributed). MHC indicates major histocompatibility complex; ON, optic nerve.

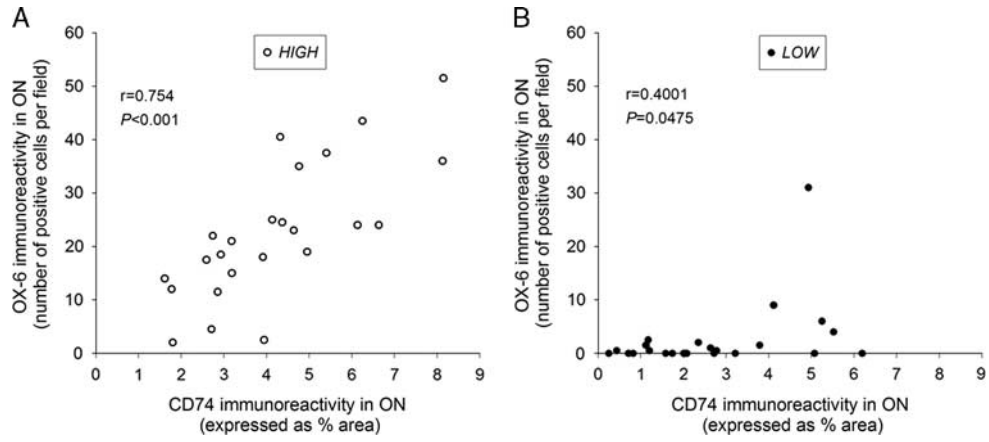

FIGURE 8. Correlation between CD74 and OX-6 immunoreactivities in longitudinal sections of the intracranial ON at 2 weeks after induction of experimental glaucoma in the High (A) and Low (B) cohorts. Each data point represents 1 animal. ON indicates optic nerve.

Copyright © 2016 Wolters Kluwer Health, Inc. All rights reserved.

elevation of IOP in 2 discrete cohorts of Sprague-Dawley rats with differing constitutive expression of MHC II RT1B. The results showed that in the cohort of rats with innately higher expression of MHC II RT1B, elevated IOP-induced axonal degeneration and RGC loss were significantly greater than in the cohort of rats with low basal expression of MHC II RT1B, despite both cohorts displaying IOP responses that were indistinguishable in terms of peak IOP and IOP integral. Iba1 and ED1, respectively, markers of total microglial number and phagocytosis, were elevated in the damaged ONs of both cohorts, with the extent of expression in each cohort reflecting the severity of axonal injury. Microglial expression of both the invariant chain of MHC II and the RT1B chain was very low in the uninjured ONs of each cohort. In the injured ONs of both cohorts, microglia upregulated expression of the invariant chain of MHC II, the extent to which correlated with the severity of axonal injury. A differential response, however, was apparent with regard to MHC II RT1B: in the cohort of rats with very low basal expression of MHC II RT1B, microglia within damaged ONs largely failed to upregulate expression of MHC II RT1B, yet, in the cohort of rats with a higher basal level of MHC II RT1B, microglia within injured ONs did upregulate expression of MHC II RT1B. Thus, it can be concluded that microglial expression of MHC II RT1B was associated with more severe axonal degeneration during experimental glaucoma.

The most important point to make when discussing the present results is that the data cannot, and should not, be viewed as providing direct evidence for a causative relationship between expression of MHC II RT1B by microglia and RGC degeneration. The definitive finding of greater RGC vulnerability to chronic IOP elevation in the cohort of rats that displayed markedly higher basal and induced expression of MHC II RT1B may simply be coincidental. Multiple genetic differences (polymorphisms resulting in allelic variation) could exist between the 2 cohorts of rats, any one of which might have played a causative role in the observed results. As an outbred stock, the Sprague-Dawley necessarily comprises populations of rats with innate genetic variation. Limited inbreeding will inevitably occur within each isolated population, which, when combined with environmental factors, also specific to each facility, will, over time, lead to further genetic drift within the individual populations of rats. Although this scenario likely accounts for the observed difference in basal and induced MHC II RT1B expression between the 2 cohorts—and it should be noted that MHC II RT1B expression following neuronal injury is particularly strain dependent[31]—it will also encompass an unknown number of other genes that could be involved in degeneration.

Although the data presented herein do not provide direct evidence of cause-effect, they do serve to focus attention on the need for research that investigates the relationship between reactive microglia and RGC injury in general, and microglial MHC II expression and RGC degeneration in particular. Our previous results,[22] and those of others,[8,13,32–34] have clearly established that axonal injury subsequent to chronically elevated IOP is associated with a spatially and temporally coordinated reactive microgliosis, the extent of which reflects the severity of injury. The microglial response is characterized by proliferation, expression of markers indicative of phagocytosis, and induction of immunologic cell surface markers, including MHC II. The present results correspond with the expected profile: in both cohorts of rats, axonal injury was associated with an increased number of microglia, an increased presence of ED1 (a marker of phagocytosis), and induction of CD74 (a marker of MHC II).

A fundamental question that has repeatedly been posed in recent years is whether microglial activation is detrimental or beneficial to RGC survival.[6] Although this issue remains unresolved, an increasing body of evidence lends support to the former scenario rather than the latter. Most pertinently, suppression of microglial activity, for example by administration of minocycline, has been shown to be neuroprotective to RGCs in models of experimental glaucoma.[10–14] Moreover, inhibition of reactive microgliosis also augments RGC survival in other injury models, such as ON transection/crush,[10,35,36] NMDA-induced excitotoxicity,[37] and ischemia-reperfusion.[38] The precise method by which minocycline protects RGCs, and, by implication, the specific mechanism(s) by which the microglia are toxic to RGCs, remain unclear, but suggested pathways of microglial toxicity include release of proinflammatory mediators and activation of the immune system.[3,6,7] In this context, it is noteworthy that minocycline has been shown to downregulate MHC II RT1B expression within spinal cord microglia and macrophages and concurrently reduce the severity of EAE symptoms.[39]

MHC II molecules expressed by activated microglia present antigenic fragments to the immune system for recognition and activation of CD4 + T cells. In autoimmune diseases of the CNS, such as EAE and multiple sclerosis, MHC II expression by activated microglia is central to the disease pathogenesis through reactivation of myelin autoreactive T cells.[19,40,41] Although glaucoma is not a classic autoimmune disease, there is some credence to the idea that autoimmunity plays a role.[42] Interestingly, however, MHC II is also implicated in the pathology of neurodegenerative conditions that are not of a primary inflammatory nature. Thus, loss of dopaminergic neurons in models of Parkinson disease is completely prevented in MHC class II knockout mice as compared with wild-type mice.[21] MHC class II knockout mice likewise show reduced CNS pathology in a model of globoid cell leukodystrophy.[20] Furthermore, strain-dependent differences in susceptibility to various CNS conditions have been linked to differential expression of the RT1B chain of MHC II. For example, in ventral root avulsion,[17] a standardized mechanical nerve trauma model, the ACI and PVG.1AV1 rat strains display low expression of MHC II RT1B by microglia and high survival of lesioned motorneurons, whereas the DA strain has high MHC II RT1B expression and low survival of lesioned motorneurons.[31,43,44]

In conclusion, the present results indicate the possibility of an association between MHC II expression and RGC degeneration in experimental glaucoma. MHC II expression after nerve injury is known to be subject to complex genetic regulation,[45] but the genetic profiles of the Sprague-Dawley cohorts in the current study remain unknown. Therefore, more targeted studies are needed to investigate the role of MHC II in experimental glaucoma. Specific experiments of interest would include comparison of RGC degeneration following induction of experimental glaucoma in rat strains with different MHC II haplotypes. Of even greater relevance would be analysis of severity of glaucomatous pathology in MHC II knockout versus wild-type mice.

ACKNOWLEDGMENT

The authors thank Mark Daymon for expert technical assistance.

REFERENCES

1. Quigley HA, Broman AT. The number of people with glaucoma worldwide in 2010 and 2020. *Br J Ophthalmol*. 2006; 90:262–267.
2. Casson RJ, Chidlow G, Wood JP, et al. Definition of glaucoma: clinical and experimental concepts. *Clin Experiment Ophthalmol*. 2012;40:341–349.
3. Chong RS, Martin KR. Glial cell interactions and glaucoma. *Curr Opin Ophthalmol*. 2015;26:73–77.
4. Seitz R, Ohlmann A, Tamm ER. The role of Muller glia and microglia in glaucoma. *Cell Tissue Res*. 2013;353:339–345.
5. Hanisch UK, Kettenmann H. Microglia: active sensor and versatile effector cells in the normal and pathologic brain. *Nat Neurosci*. 2007;10:1387–1394.
6. Johnson EC, Morrison JC. Friend or foe? Resolving the impact of glial responses in glaucoma. *J Glaucoma*. 2009;18: 341–353.
7. Wang JW, Chen SD, Zhang XL, et al. Retinal microglia in glaucoma. *J Glaucoma*. 2016;25:459–465.
8. Bosco A, Steele MR, Vetter ML. Early microglia activation in a mouse model of chronic glaucoma. *J Comp Neurol*. 2011;519: 599–620.
9. Bosco A, Romero CO, Breen KT, et al. Neurodegeneration severity is anticipated by early microglia alterations monitored in vivo in a mouse model of chronic glaucoma. *Dis Model Mech*. 2015;8:443–455.
10. Levkovitch-Verbin H, Kalev-Landoy M, Habot-Wilner Z, et al. Minocycline delays death of retinal ganglion cells in experimental glaucoma and after optic nerve transection. *Arch Ophthalmol*. 2006;124:520–526.
11. Bosco A, Inman DM, Steele MR, et al. Reduced retina microglial activation and improved optic nerve integrity with minocycline treatment in the DBA/2J mouse model of glaucoma. *Invest Ophthalmol Vis Sci*. 2008;49: 1437–1446.
12. Wang K, Peng B, Lin B. Fractalkine receptor regulates microglial neurotoxicity in an experimental mouse glaucoma model. *Glia*. 2014;62:1943–1954.
13. Bosco A, Crish SD, Steele MR, et al. Early reduction of microglia activation by irradiation in a model of chronic glaucoma. *PLoS One*. 2012;7:e43602.
14. Howell GR, Soto I, Zhu X, et al. Radiation treatment inhibits monocyte entry into the optic nerve head and prevents neuronal damage in a mouse model of glaucoma. *J Clin Invest*. 2012;122:1246–1261.
15. Perry VH. A revised view of the central nervous system microenvironment and major histocompatibility complex class II antigen presentation. *J Neuroimmunol*. 1998;90: 113–121.
16. Harnesk K, Swanberg M, Ockinger J, et al. Vra4 congenic rats with allelic differences in the class II transactivator gene display altered susceptibility to experimental autoimmune encephalomyelitis. *J Immunol*. 2008;180:3289–3296.
17. Piehl F, Swanberg M, Lidman O. The axon reaction: identifying the genes that make a difference. *Physiol Behav*. 2007;92:67–74.
18. Dominguez CA, Lidman O, Hao JX, et al. Genetic analysis of neuropathic pain-like behavior following peripheral nerve injury suggests a role of the major histocompatibility complex in development of allodynia. *Pain*. 2008;136:313–319.
19. Tompkins SM, Padilla J, Dal Canto MC, et al. De novo central nervous system processing of myelin antigen is required for the initiation of experimental autoimmune encephalomyelitis. *J Immunol*. 2002;168:4173–4183.
20. Matsushima GK, Taniike M, Glimcher LH, et al. Absence of MHC class II molecules reduces CNS demyelination, microglial/macrophage infiltration, and twitching in murine globoid cell leukodystrophy. *Cell*. 1994;78:645–656.
21. Harms AS, Cao S, Rowse AL, et al. MHCII is required for alpha-synuclein-induced activation of microglia, CD4 T cell proliferation, and dopaminergic neurodegeneration. *J Neurosci*. 2013;33:9592–9600.
22. Ebneter A, Casson RJ, Wood JP, et al. Microglial activation in the visual pathway in experimental glaucoma: spatiotemporal characterization and correlation with axonal injury. *Invest Ophthalmol Vis Sci*. 2010;51:6448–6460.
23. Levkovitch-Verbin H, Quigley HA, Martin KR, et al. Translimbal laser photocoagulation to the trabecular meshwork as a model of glaucoma in rats. *Invest Ophthalmol Vis Sci*. 2002;43: 402–410.
24. Chidlow G, Daymon M, Wood JP, et al. Localization of a wide-ranging panel of antigens in the rat retina by immunohistochemistry: comparison of Davidson's solution and formalin as fixatives. *J Histochem Cytochem*. 2011;59:884–898.
25. Chidlow G, Ebneter A, Wood JP, et al. The optic nerve head is the site of axonal transport disruption, axonal cytoskeleton damage and putative axonal regeneration failure in a rat model of glaucoma. *Acta Neuropathol*. 2011;121:737–751.
26. Ebneter A, Chidlow G, Wood JP, et al. Protection of retinal ganglion cells and the optic nerve during short-term hyperglycemia in experimental glaucoma. *Arch Ophthalmol*. 2011; 129:1337–1344.
27. Ebneter A, Casson RJ, Wood JP, et al. Estimation of axon counts in a rat model of glaucoma: comparison of fixed-pattern sampling with targeted sampling. *Clin Experiment Ophthalmol*. 2012;40:626–633.
28. Kim MK, Palestine AG, Nussenblatt RB, et al. Expression of class II antigen in endotoxin induced uveitis. *Curr Eye Res*. 1986;5:869–876.
29. Pease ME, Zack DJ, Berlinicke C, et al. Effect of CNTF on retinal ganglion cell survival in experimental glaucoma. *Invest Ophthalmol Vis Sci*. 2009;50:2194–2200.
30. Bull ND, Irvine KA, Franklin RJ, et al. Transplanted oligodendrocyte precursor cells reduce neurodegeneration in a model of glaucoma. *Invest Ophthalmol Vis Sci*. 2009;50:4244–4253.
31. Lundberg C, Lidman O, Holmdahl R, et al. Neurodegeneration and glial activation patterns after mechanical nerve injury are differentially regulated by non-MHC genes in congenic inbred rat strains. *J Comp Neurol*. 2001;431:75–87.
32. Howell GR, Libby RT, Jakobs TC, et al. Axons of retinal ganglion cells are insulted in the optic nerve early in DBA/2J glaucoma. *J Cell Biol*. 2007;179:1523–1537.
33. Johnson EC, Jia L, Cepurna WO, et al. Global changes in optic nerve head gene expression after exposure to elevated intraocular pressure in a rat glaucoma model. *Invest Ophthalmol Vis Sci*. 2007;48:3161–3177.
34. Lam TT, Kwong JM, Tso MO. Early glial responses after acute elevated intraocular pressure in rats. *Invest Ophthalmol Vis Sci*. 2003;44:638–645.
35. Baptiste DC, Powell KJ, Jollimore CA, et al. Effects of minocycline and tetracycline on retinal ganglion cell survival after axotomy. *Neuroscience*. 2005;134:575–582.
36. Wang J, Chen S, Zhang X, et al. Intravitreal triamcinolone acetonide, retinal microglia and retinal ganglion cell apoptosis in the optic nerve crush model. *Acta Ophthalmol*. 2015. [Epub ahead of print].
37. Shimazawa M, Yamashima T, Agarwal N, et al. Neuroprotective effects of minocycline against in vitro and in vivo retinal ganglion cell damage. *Brain Res*. 2005;1053:185–194.
38. Mathalone N, Lahat N, Rahat MA, et al. The involvement of matrix metalloproteinases 2 and 9 in rat retinal ischemia. *Graefes Arch Clin Exp Ophthalmol*. 2007;245:725–732.
39. Nikodemova M, Watters JJ, Jackson SJ, et al. Minocycline down-regulates MHC II expression in microglia and macrophages through inhibition of IRF-1 and protein kinase C (PKC)alpha/betaII. *J Biol Chem*. 2007;282:15208–15216.
40. Slavin AJ, Soos JM, Stuve O, et al. Requirement for endocytic antigen processing and influence of invariant chain and H-2M deficiencies in CNS autoimmunity. *J Clin Invest*. 2001;108: 1133–1139.
41. Flugel A, Berkowicz T, Ritter T, et al. Migratory activity and functional changes of green fluorescent effector cells before

and during experimental autoimmune encephalomyelitis. *Immunity*. 2001;14:547–560.
42. Bell K, Gramlich OW, Von Thun Und Hohenstein-Blaul N, et al. Does autoimmunity play a part in the pathogenesis of glaucoma? *Prog Retin Eye Res*. 2013;36:199–216.
43. Piehl F, Lundberg C, Khademi M, et al. Non-MHC gene regulation of nerve root injury induced spinal cord inflammation and neuron death. *J Neuroimmunol*. 1999;101:87–97.
44. Lidman O, Swanberg M, Horvath L, et al. Discrete gene loci regulate neurodegeneration, lymphocyte infiltration, and major histocompatibility complex class II expression in the CNS. *J Neurosci*. 2003;23:9817–9823.
45. Diez M, Abdelmagid N, Harnesk K, et al. Identification of gene regions regulating inflammatory microglial response in the rat CNS after nerve injury. *J Neuroimmunol*. 2009;212: 82–92.